

Sequence analysis

TEtranscripts: a package for including transposable elements in differential expression analysis of RNA-seq datasets

Ying Jin, Oliver H. Tam, Eric Paniagua and Molly Hammell*

Cold Spring Harbor Laboratory, Cold Spring Harbor, NY, 11724, USA

*To whom correspondence should be addressed.

Associate Editor: Ivo Hofacker

Received on February 19, 2015; revised on June 22, 2015; accepted on July 14, 2015

Abstract

Motivation: Most RNA-seq data analysis software packages are not designed to handle the complexities involved in properly apportioning short sequencing reads to highly repetitive regions of the genome. These regions are often occupied by transposable elements (TEs), which make up between 20 and 80% of eukaryotic genomes. They can contribute a substantial portion of transcriptomic and genomic sequence reads, but are typically ignored in most analyses.

Results: Here, we present a method and software package for including both gene- and TE-associated ambiguously mapped reads in differential expression analysis. Our method shows improved recovery of TE transcripts over other published expression analysis methods, in both synthetic data and qPCR/NanoString-validated published datasets.

Availability and implementation: The source code, associated GTF files for TE annotation, and testing data are freely available at <http://hammelllab.labsites.cshl.edu/software>.

Contact: mhammell@cshl.edu.

Supplementary information: [Supplementary data](#) are available at *Bioinformatics* online.

1 Introduction

Transposable elements are mobile DNA elements that constitute a large fraction of most eukaryotic genomes. These parasitic genetic elements propagate by multiplying within the genomes of host cells and can be passed from generation to generation through the germline lineage. Although the majority of TE copies are non-functional, a subset has retained the ability to transcribe and mobilize (Beck *et al.*, 2010; Bennett *et al.*, 2008; Hancks and Kazazian, 2012; Honma *et al.*, 1993; Huang *et al.*, 2012; Kano *et al.*, 2009; Mills *et al.*, 2007). Although retrotransposons require an RNA intermediate to transpose, both DNA and RNA transposons are transcribed from the genome, and they can accumulate in conditions such as cancer (Criscione *et al.*, 2014; Lamprecht *et al.*, 2012; Lee *et al.*, 2012; Sciamanna *et al.*, 2013; Sciamanna *et al.*, 2014; Shukla *et al.*, 2013; Tubio *et al.*, 2014), neurodegenerative diseases (Bundo *et al.*, 2014; Li *et al.*, 2013; Reilly *et al.*, 2013), as well as during embryogenesis (Fadloun *et al.*, 2013; Macia *et al.*, 2011; Peaston *et al.*, 2004), neural development

(Coufal *et al.*, 2009; Coufal *et al.*, 2011; Faulkner *et al.*, 2009; Muotri *et al.*, 2005; Perrat *et al.*, 2013; Thomas *et al.*, 2012) and aging (De Cecco *et al.*, 2013; Li *et al.*, 2013; Sedivy *et al.*, 2013). However, TE-associated reads are often discarded in sequencing data analyses because of the uncertainty in attributing ambiguously mapped reads to these regions, despite some previous attempts to integrate them in downstream analyses (Chung *et al.*, 2011; Day *et al.*, 2010; Rosenfeld *et al.*, 2009; Treangen and Salzberg, 2011; Tucker *et al.*, 2011; Wang *et al.*, 2010). Here, we present a program called *TEtranscripts* that allows users to analyze both gene- and TE-associated reads concurrently in one simplified workflow.

2 Input data

The input data for *TEtranscripts* consists of alignment files in either the SAM or BAM format (Li *et al.*, 2009), and two annotation files in the General Transfer Format (GTF) (<http://mblab.wustl.edu/GTF22>).

html) for genes and TEs, respectively. For the purposes of this article, we will use the terms, unique-reads and multi-reads, to designate the reads that have a unique alignment in the genome or map to multiple loci with equal quality, respectively. The utilization of multi-reads for TE quantification is critical, as a read originating from a TE could align to multiple instances (insertions) of that element in the genome. Many aligners support multi-reads alignments, and provide limits for the maximum number of multiple alignments per reads to output, e.g. *bowtie -m* (Langmead et al., 2009). To optimally set this parameter, we recommend a saturation analysis on the multi-read alignments as described in the [Supplementary Materials](#) (Supplementary Fig. S1). *TEtranscripts* also supports strand-specific read counting, and applies it to both genes and TEs. GTF files of transposable element annotations were generated from the RepeatMasker (Smit et al., 1996, <http://www.repeatmasker.org>) tables obtained from the UCSC genome database (Karolchik et al., 2003), or from annotations provided by the maize MIPS (Nussbaumer et al., 2013) and MTEC databases (<http://maizetdb.org/~maize/>). The annotation tables were parsed to filter out low complexity and simple repeats, rRNA, scRNA, snRNA, srpRNA and tRNA. Each TE insertion in the table was given a unique identifier. The genomic location, element name, as well as family and class information were also extracted from the table and included in the GTF file. *TEtranscripts* can also utilize custom TE annotations, such as those generated from *de novo* TE insertion analysis, as long as they conform to the format described earlier and are consistent with the genome sequencing files used for the alignment.

3 Methods

TEtranscripts estimates both gene and TE transcript abundances in RNA-seq data and conducts differential expression analysis on the resultant count tables. The general workflow of *TEtranscripts* is given in Figure 1. Read assignment and statistical modeling is discussed in detail in this section.

3.1 Index genomic features

To quickly find all genes/TEs that overlap with any given read alignment, *TEtranscripts* builds two independent index structures on gene and TE annotations, respectively. The gene/TE index structure consists of a hash table with reference sequence names and a list of

interval trees as key-value pairs. For each chromosome, there is an interval tree generated based on gene/TE insertions annotated on that chromosome. It allows the SAM/BAM read alignment to be rapidly matched with the genome intervals in GTF annotations, especially when there are a large number of TE insertions.

3.2 Read assignment

The next step involves distributing the mapped reads among the annotated genes and TEs that overlap those genomic alignments. Unique-reads, which represent most gene-associated reads, but only a subset of TE-associated reads, are comparatively simple to distribute. For a multi-read, the task is more difficult. *TEtranscripts* takes advantage of the sequence similarities at the different levels of the hierarchy of TEs in order to optimally distribute reads amongst closely related TE sequences. Based on the definitions and nomenclature provided by RepBase (Jurka et al., 2005), TE ‘insertions’ (loci within the genome) are grouped into ‘elements’, which are sub-families of TEs that are highly related at the sequence level and relatively distinct from other elements. For example, Repbase and RepeatMasker report 16 293 insertions for the *L1Md_A* element in the mouse reference genome (mm9), all of which are more similar to each other than they are to other elements of the *L1* family (such as *L1Md_T*). By estimating combined abundances for all insertions of an element, we obtain more reliable and reproducible results than analyses that attempt to pin down the exact genomic instance of the TE being transcribed. Thus, *TEtranscripts* performs estimation of expression abundances on the element level by default, which is the recommended setting. *TEtranscripts* parses the alignment file only once, processing genes and TEs at the same time. Given a uniquely mappable read, the algorithm first searches for overlapping gene exons; if it is a multi-read, overlap with TEs will be first computed. For TE-associated reads, the user can choose whether to count only unique-reads or all reads, i.e. *uniq* mode and *multi* mode.

Under *multi* mode, it is important to assign weight to the contribution of the ambiguously mapped reads at each mapped locus, so that no double counting of reads occurs. Given all available alignments of a read, every alignment is assigned a weight of $1/n$, where n is the number of alignments. Therefore, the total contribution of a multi-read to the library size is the same as a unique-read. This is important in maintaining the library size for each sample (calculated based on the total number of mapped reads), as it is heavily utilized for normalization when comparing between multiple libraries.

3.3 TE transcript estimation

After the read assignment step, an expectation-maximization (EM) algorithm is used to determine the maximum-likelihood estimates of multi-reads assignments to all TE transcripts. The unique-reads are not used as a prior for the initial abundance estimates in the EM procedure to reduce potential bias to certain TEs. Specifically, active TEs, which tend to be younger elements, have accumulated far fewer polymorphisms than older TEs, and thus have far fewer reads mapping uniquely to these elements. Using uniquely mapped TE reads in the optimization step will bias read assignment away from the youngest TE sub-families and toward the older related TE subfamilies with higher uniquely mappable content.

3.3.1 Expectation maximization

The EM algorithm alternates between computing the fractional distribution of each multi-read to each mapped TE instance (E-step) and estimating the relative abundances of all TE transcripts (M-step), until the estimated relative abundances converge. The initial

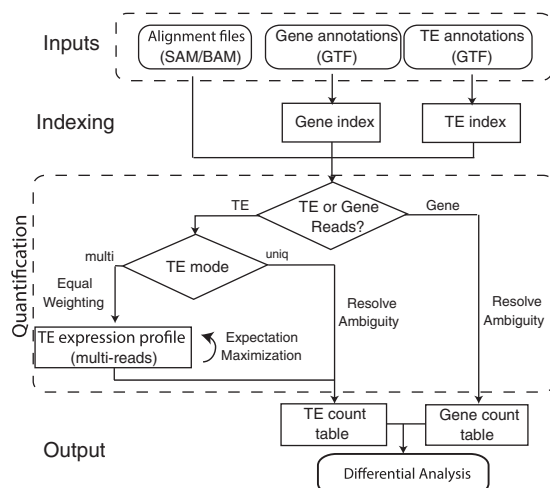


Fig. 1. *TEtranscripts* flow chart. Reads mapping to TEs are assigned in two different modes: *uniq* (reads mapping uniquely in the genome), and *multi* (reads mapping to multiple insertions of TEs). In the *multi* mode, an iterative algorithm is used to optimally distribute ambiguously mapped reads

estimation of relative abundance on multi-reads, ρ , of each TE transcript, t , is computed by Equation (1).

$$\rho_t^0 = \frac{F_t}{\sum_{s \in T} F_s} \quad (1)$$

T is the set of all TE transcripts; F_t is the set of multi-reads assigned to t ; \tilde{l}_t denotes the effective length of transcript t , $\tilde{l}_t = l_t - m + 1$, where m is the fragment length and l_t is the length of transcript t . The fragment length is calculated from the paired-end alignment input file, or provided as a parameter by the user for single-end samples.

The E-step computes the fraction of each multi-read allocated to each TE transcript. Suppose that a multi-read f maps to a set of TE transcripts T_i . According to the initial assignment, the fraction of f attributed to any TE transcript t in T_i , $\alpha^0(f, t)$, is the relative abundance of t over the sum of relative abundance of all TE transcripts in T_i , $\alpha^0(f, t) = \frac{\rho_t^0}{\sum_{t' \in T_i} \rho_{t'}^0}$. This allocation will then be used in the M-step of the algorithm to compute the relative abundance of each TE transcript. As described in Equations (2) and (3), these two steps will run alternatively for a specified number of iterations, k , until the program converges or as set by the user.

$$\alpha^k(f, t) = \frac{\rho_t^{(k-1)}}{\sum_{t' \in T_i} \rho_{t'}^{(k-1)}} \quad (2)$$

$$\rho_t^k = \frac{\sum_{f \rightarrow t} \alpha^k(f, t)}{\sum_{s \in T} \sum_{f' \rightarrow s} \alpha^k(f', s)} \quad (3)$$

After the EM procedure, the estimated relative abundance of each TE transcript from the multi-reads is integrated with the unique-read counts to compute the total relative abundance. The element level abundances are then computed by summing up all instances of each TE subfamily.

3.4 Differential analysis

Following the generation of a count table for gene and TE transcripts, the differential expression analysis closely follows the DESeq package (Anders and Huber, 2010) for modeling the counts data with a negative binomial distribution and computing adjusted P -values. In addition to the standard transcript abundance normalization approach used by the DESeq package, *TEtranscripts* offers two additional options, reads per mapped million (RPM) and Quantile normalization. All other procedures exactly follow the DESeq method. *TEtranscripts* runs the DESeq method with a default set of general parameters. When there are no (or very few) replicates, we use the *blind* method for variance estimation and *fit-only* for SharingMode. Otherwise, we use *pooled* or *per-condition* methods and *maximum* SharingMode, as suggested by the DESeq package. In all scenarios, we use the *parametric* fitting model (fitType). The R code used for differential expression analysis is generated as part of the output to allow users to further customize the DESeq parameters and re-calculate differential expression statistics.

3.5 Implementation

TEtranscripts is written in Python. The SQUAREM (Varadhan and Roland, 2008) procedure is used during EM iterations to improve

the convergence speed. *TEtranscripts* is available as an open-source program under a standard GPLv3 open source license and has been developed and tested on Linux and Macintosh OSX. The software package and associated TE GTF files can be found at <http://hammelllab.labsites.cshl.edu/software>. The TE GTF files currently include chimpanzee (panTro4), fly (dm3), maize (Zea mays RefGen v2), mouse (mm9 and mm10), rat (rn5 and rn6) and human (hg18, hg19/GRCh37, and hg38/GRCh38).

4 Results

To examine the accuracy and performance of *TEtranscripts*, we compared it with HTSeq-count version 0.5.4p3 (Anders et al., 2014), Cufflinks version v2.1.1 (Trapnell et al., 2010, 2012) and RepEnrich (Criscione et al., 2014) on both synthetic and real data. HTSeq-count was chosen as a standard method that counts only uniquely mapped reads and is nearly identical to the *uniq* mode in *TEtranscripts*. Cufflinks was chosen as a popular method for gene abundance estimation that works from pre-mapped BAM files and includes options to handle multi-reads, but is not specifically designed for TEs. To the best of our knowledge, only one other published method has been designed for TE expression analysis from RNA-seq data, RepEnrich, but this method does not work with pre-mapped BAM files. There is a recently published pipeline set piPipes (Han et al., 2015) to study piRNAs and TE-derived RNAs. Because it uses HTSeq-count and Cufflinks for quantification and Cuffdiff for differential analysis, we did not include comparisons to piPipes separately.

For all comparisons, TE abundance measurements were given at the resolution of the element level (e.g. *L1Md_A*). For the synthetic datasets, accuracy was quantified as the proportion of abundances accurately recovered by each method for each TE element. For published datasets, accuracy was determined by agreement between the quantitative validation measurements (e.g. Q-PCR, NanoString) and the expression estimations computed by each software package.

4.1 TE recovery in synthetic data

Simulated datasets were used to investigate the TE abundance recovery rate by each approach, paying particular attention to the recovery of TEs known to be active in the mouse genome, obtained from a study by Molaro et al. (2014). FluxSimulator v1.2.1 (Griebel et al., 2012) was used to generate multiple RNA-seq datasets from the mouse genome (mm9), consisting of 76 bp single-end reads from transcripts that include both annotated genes and TEs (see Supplementary Table S1 for parameters used). Each dataset consisted of 24 million reads in total, with 17% of all transcripts derived from TEs of varying abundances. STAR (Dobin et al., 2012) was used to map the simulated reads with maximum multiple alignments of no more than 100, using the variables `-winAnchorMultimapNmax 100` and `-outFilterMultimapNmax 100`. Based on these parameters, we found that 87% of the reads were mapped onto the mouse genome, while TE reads had an average mappability of 70%. Furthermore, roughly half of the TE reads generated were uniquely mappable, comparable to what is observed in published transcriptome datasets. The simulated TE reads had a smaller mappability rate than gene-associated reads largely due to reads aligning to more than 100 genomic locations.

The aligned read files were then used as input for the four abundance estimation approaches used in this study: HTSeq-count, Cufflinks, RepEnrich, and *TEtranscripts*. HTSeq-count was run in *intersection-nonempty* mode, and using a GTF file that contains

both TE and gene annotations for abundance estimation. Because HTSeq-count considers only uniquely mapped reads, any multi-mapped TE reads will be discarded by this approach. Cufflinks was run with the settings of rescue method for multi-reads ($-u$), which takes into account both unique-reads and multi-reads, and uniformly divide each multi-read to all the positions initially. When multi-read correction is enabled, Cufflinks will reassign each multi-mapped read probabilistically based on the initial abundance estimations, with the uniquely mapping reads used to inform the likely distribution of the multi-reads (Trapnell et al., 2010, 2012). To run RepEnrich, we built the pseudogenome of TEs using the RepeatMasker file on mm9 as described in the RepEnrich tutorial. Unique-reads and multi-reads were derived based on the STAR output. *TEtranscripts* was run in *multi* mode with EM optimization invoked. The accuracy of each method in estimating abundances of TE expression was computed and displayed as the frequencies of the rate of recovered abundances (Fig. 2; Supplementary Fig. S2).

In general, *TEtranscripts* outperforms HTSeq-count, Cufflinks and RepEnrich in terms of abundance recovery rate, both for non-functional and active TEs. The overall average recovery rate for *TEtranscripts* was 88.84%, with 53.74% for HTSeq-count, 43.72% for Cufflinks and 59.8% for RepEnrich. The fraction of TEs for which the estimated abundance is within 15% of the true abundance was: 41.7% for *TEtranscripts*, 14.4% for HTSeq-count, 9.3% for RepEnrich and 16.8% for Cufflinks. In this dataset, 14.5% of the detected TEs are active TEs, and all three approaches were able to capture some of them. *TEtranscripts* was able to recover >80% of the reads for 77% of the active TEs; HTSeq-count was not able to recover >80% of the reads for any of the active elements; Cufflinks recovered at least 80% of the reads for 8% of the active TEs; RepEnrich recovered >80% of reads for 75% of the active TEs, but over-counted 57.69% of the active TEs. The fraction of active TEs for which the estimated abundance is within 15% of the true abundance was: 61.5% for *TEtranscripts*, 0% for HTSeq-count, 23.1% for RepEnrich, and 3.8% for Cufflinks. *TEtranscripts* and

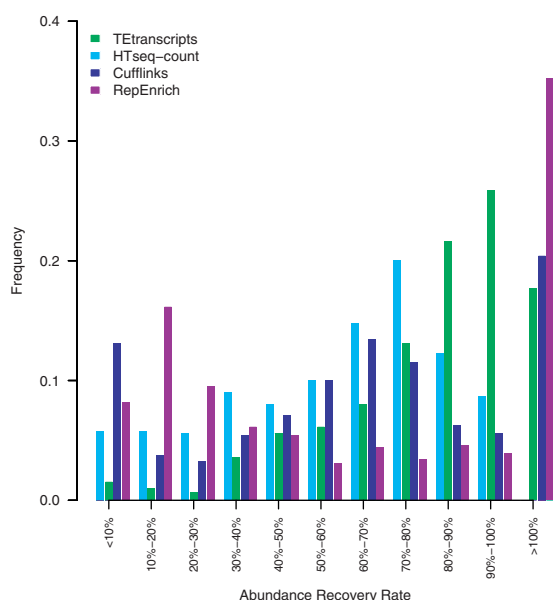


Fig. 2. Comparison of TE abundance recovery. Displayed are the distributions of the rate of measured abundances versus true abundances by each method. HTSeq-count abundance recovery rates shown in light blue, Cufflinks recovery rates shown in blue, *TEtranscripts* with *multi* mode recovery rates shown in green, and RepEnrich recovery rates shown in purple

RepEnrich over-counted some TEs, which is displayed as the 15% of elements whose abundances were estimated to be >100% of their actual values at the far right of Figure 2. Please refer to Supplementary Figure S4 for recovery rates with and without the EM optimization option in *TEtranscripts*.

Figure 3 shows the abundances of active TEs estimated by each software package as compared with the ground truth (denoted with red dots). In most cases, *TEtranscripts* (green dots) is within 90% of the actual value, while the other two methods, HTSeq-count and Cufflinks, frequently under-estimate the abundance of TE transcripts for young, active TEs. RepEnrich (purple dots) shows more variations, nearly 30% under-estimation and 40% over-estimation. HTSeq-count (light blue dots) was expected to underestimate the counts, since the discarded multi-reads often constitute nearly 50% of the TE-associated reads. Surprisingly, Cufflinks also under-estimates the abundances for many active TEs, despite incorporating multi-reads in its analysis. Both under- and over-estimating the TE transcript abundances will affect both the ability to accurately calculate fold changes between samples and the power with which to calculate *P*-values for any associated changes. Please refer to Supplementary Figure S3 for the distribution of abundance recovery rates on active TEs of four approaches. In the next section, we assess the ability of these methods to return accurate fold changes and significant *P*-values for TEs known to have altered expression in published datasets that used a quantitative validation of their RNA-seq data.

4.2 TE recovery in published data

To determine the usefulness of our algorithm on experimentally generated results, we tested *TEtranscripts* on previously published RNA-seq datasets of *Drosophila* and mouse transcriptomes. We then compared *TEtranscripts* to other approaches, such as HTSeq-count, Cufflinks and RepEnrich, each combined with DESeq. We applied DESeq for differential expression analysis on the outputs of the three approaches to directly compare the effects of quantification on *P*-value estimation. Both HTSeq-count and RepEnrich output raw counts that can be input to DESeq without transformation. The output of Cufflinks has to be converted to raw counts before running DESeq. To convert Cufflinks output, we first calculated raw counts assigned to each isoform by multiplying the length over 1000 to the Fragments Per Kilobase of exon per Million reads

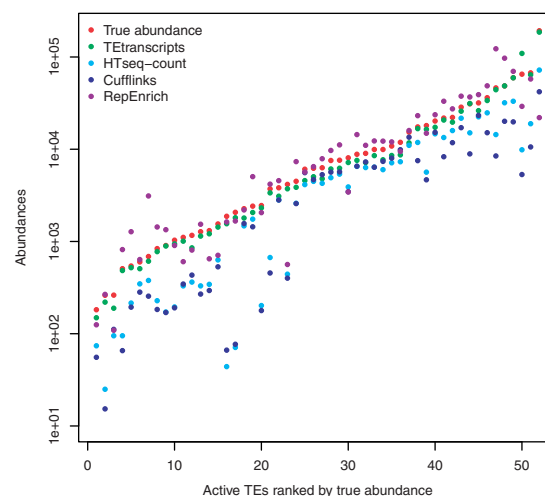


Fig. 3. Active TE expression estimation. Reads associated with active TE elements are more likely to be missed by algorithms that rely heavily on unique reads

mapped (FPKM) value of each isoform, and then summarized them on genes or transposable elements.

Although the Cufflinks package includes its own differential expression analysis software, Cuffdiff, it required at least 550 GB of memory to run on these datasets, and performed no better in terms of fold change estimation or *P*-value concordance than the results displayed below (Supplementary Fig. S5).

4.2.1 *Drosophila melanogaster* transcriptome

The *Drosophila* dataset comes from a study by Ohtani *et al.* (2013) that observed the de-repression of transposable elements upon alteration of DmGTSF1, which works with the Piwi-associated silencing complex (piRISC) to silence TEs in the *Drosophila* ovary. This dataset was chosen because they assessed TE expression levels with RNA-seq, followed by validation through Q-PCR. This will allow us to compare the estimated fold changes from the four approaches, HTSeq-count, Cufflinks, RepEnrich, and *TEtranscripts*, with their Q-PCR results. We obtained the raw FASTQ data from Gene Expression Omnibus (accession no. GSE47006) and mapped with STAR, as described earlier, onto the *D. melanogaster* genome (dm3). Although *TEtranscripts*, HTSeq-count and Cufflinks were able to perform quantification directly from the BAM alignment output, RepEnrich requires independent alignment and TE quantification. We built a pseudogenome for dm3 TEs using the RepeatMasker open-4.0.5 release file (Smit *et al.*, 1996) download from the following link: <http://www.repeatmasker.org/species/dm.html>.

Figure 4 shows the TE expression changes between Piwi knock-down and wild type. The log₂ fold change (log₂FC) calculated by *TEtranscripts* in *multi* mode closely resembles the Q-PCR results in most of the TEs interrogated. HTSeq-count performs well on most elements, but not as well as *TEtranscripts* on others (e.g. *mdg1*). Cufflinks reports similar values to HTSeq-count for most TEs, but performs better than *TEtranscripts* and HTSeq-count on the *roo* element. Surprisingly, RepEnrich deviates substantially from the qPCR validation results, and DESeq identified no differentially expressed TEs.

4.2.2 Mouse transcriptome

In order to evaluate the utility of *TEtranscripts* on a mammalian genome with higher TE content, we selected a recently published

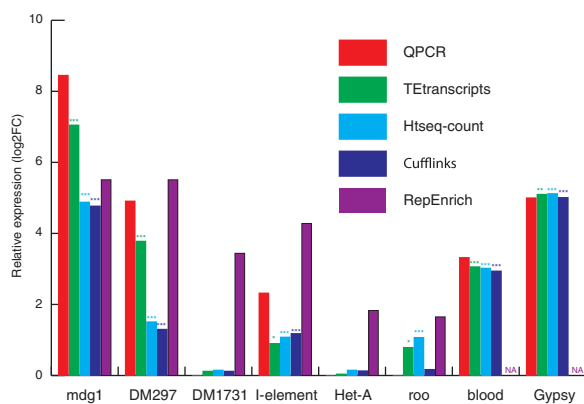


Fig. 4. Comparing *Drosophila* TE expression estimation. *TEtranscripts* was compared with HTSeq-count, Cufflinks, and RepEnrich. Log₂ fold changes of Piwi knock-down versus wild type are shown here. 'NA' denotes circumstances where expression could not be estimated. The asterisk symbol represents the level of significances, '****' adjusted *P*-value < 1e – 5, '***' adjusted *P*-value < 0.01, '**' adjusted *P*-value < 0.05

study in mouse from Gnanakkan *et al.* (2013). In this study, they provided NanoString quantification of several TEs, comparing a previously published RNA-seq dataset (GEO accession number GSE30352) (Brawand *et al.*, 2011), to their microarray-based tool, TE-array. We performed similar analyses as described in the previous section, except that we map the reads to the mouse genome (mm10) and mouse TE pseudogenome (for RepEnrich).

Figure 5 shows the comparison between *TEtranscripts* with *multi* mode and other quantification approaches. Similar to the results on *Drosophila* data, *TEtranscripts* outperforms HTSeq-count on many TEs (e.g. *L1_{Mm}*, *ERBV4*, *MMVL30* and *ERVB2*). Cufflinks (in multi-reads rescue mode) performs comparably with *TEtranscripts* on some TEs, but often fails to return abundance counts on others (as indicated by 'NA' in the plot). RepEnrich again deviates from the expected values (nanoString), and fails to identify any differentially expressed TEs from its quantification results.

4.2.3 TEtranscripts quantification in other published studies

Finally, the methodology utilized in *TEtranscripts* has also been applied in studying transposable elements mis-regulation in TDP-43-mediated neurodegenerative disorders (Li *et al.*, 2013) and the roles of Piwi in the piRNA pathway and transposon repression (Rozhkov *et al.*, 2013). In both studies, we were able to demonstrate significant differential expression of TEs that was consistent with the biological phenotypes and with the set of TEs altered in independent experiments for those studies.

4.3 Running time and memory usage

We tested the running time and memory usage of *TEtranscripts* on simulated RNA-seq data. A variety of library sizes ranging from 20 to 100 M reads were generated based on the mouse genome (mm9), with each sample having 10% of the reads coming from TEs. Although *TEtranscripts* takes additional time and memory to distribute reads between the millions of TE instances in the genome as compared with other gene expression analysis packages, it is still relatively efficient, with a typical memory requirement of 8 GB and run times on the order of 1–2.5 h for datasets with 20–100 million reads per sample (Fig. 6). All the experiments were run on a server with 128 GB memory and Xeon E5-2665 processors running at

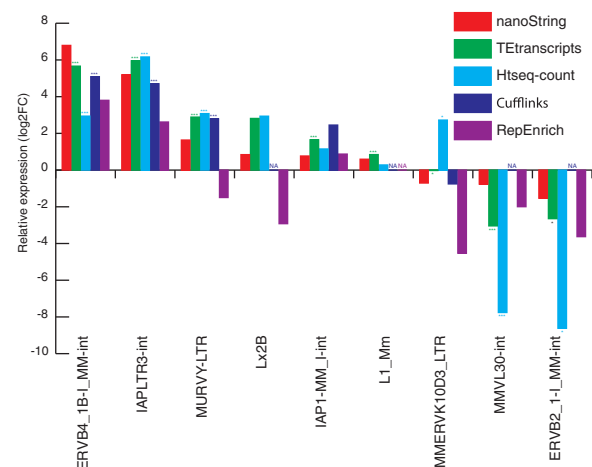


Fig. 5. Comparing mouse TE expression estimation. We selected TEs that show significant differential expression between testis and somatic tissues. The somatic tissue sample is the integration of RNA-seq data from multiple organs: liver, heart, brain and kidney. The same figure legend was used as Figure 4

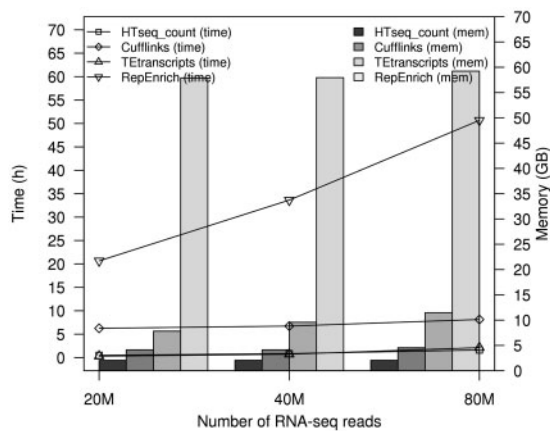


Fig. 6. Running time and memory usage. RepEnrich has a pre-requisite preparation step of building the pseudogenome of transposable elements, which was not included in this plot

2.40 GHz (16 cores). The running time was measured using the built-in bash *date* command.

5 Discussion

Transcripts derived from TEs form a small but important subset of all transcriptomic datasets. Often thought of as junk transcripts with little importance for biological phenotypes, TEs can play a large and unexpected role in important processes such as stem cell identity and reprogramming (Kelley and Rinn, 2012; Lu et al., 2014; Ohnuki et al., 2014; Wang et al., 2014), and in human diseases (Bundo et al., 2014; Lamprecht et al., 2012; Li et al., 2013; Reilly et al., 2013; Sciamanna et al., 2013, 2014; Shukla et al., 2013; Tucker et al., 2011). Although TE-derived transcripts should be included as part of standard expression analyses, there have previously been few tools that allow the easy inclusion of TE-associated reads. *TEtranscripts* allows users to simultaneously analyze gene- and TE-derived transcripts in a simple expression analysis framework that works with aligned (BAM) files and annotation files (GTF).

Using simulated reads as well as published datasets that include independent validations, we have shown that *TEtranscripts* outperforms all other published methods in abundance estimation, and concordance between statistical significance estimation and validated alterations in expression. In simulated datasets, we show that *TEtranscripts* performs particularly well at estimating the abundance of young TEs, which are more likely to be mobile and active in cells. In published datasets for both fly and mouse genomes, we show that alterations in TE expression estimated from RNA-seq data by *TEtranscripts* show better overall concordance with external validation data. *TEtranscripts* particularly outperforms other methods for complex mammalian genomes, such as the mouse, which has many more insertions per TE than flies, and a larger diversity in TE families.

As with all approaches that quantify RNA expression from alignment data, *TEtranscripts* is highly dependent on the quality of the genomic alignment and annotation data (for genes and transposable elements). This is especially problematic when working with strains or cultivars whose DNA sequences and transposable element content have diverged significantly from the ‘reference’ genome and annotations. *TEtranscripts* mitigates this limitation by providing flexibility in the input files provided by the user. Our software is agnostic to the genomic aligner and mapping parameters used to

generate the input alignment files, as long as it complies with the SAM/BAM format. This enables users to optimize genome alignment parameters according to the characteristics of their experimental system before analysis with *TEtranscripts*. *TEtranscripts* can also utilize user-defined annotations for both gene and transposable elements during quantification. Although we have provided transposable element annotation files for a few common genomes, our software will process any TE annotations in the GTF format described earlier. These could include TE annotations that have been manually curated for a specific strain, or those identified by bioinformatics tools searching for de-novo transposable elements. This will allow users to provide the best annotation data suitable for their experiment, and maximizes the quality of analysis produced by *TEtranscripts*.

Acknowledgement

We would like to thank Josh Dubnau and members of his lab for helpful discussions. We would also like to thank the Bioinformatics Shared Resource at Cold Spring Harbor Laboratory, which is supported by the National Institutes of Health.

Funding

This work was supported by the Rita Allen Foundation, of which MH is a scholar, and by a grant from the National Science Foundation [MCB-1159098 to MH]. This work was also supported by a CSHL Cancer Center Support Grant from the National Institutes of Health (NIH-NCI-CA-045508).

Conflict of Interest: none declared.

References

- Anders, S. and Huber, W. (2010) Differential expression analysis for sequence count data. *Genome Biol.*, **11**, R106.
- Anders, S. et al. (2014) Htseq—a python framework to work with high-throughput sequencing data. *Bioinformatics*, **31**, 166–169.
- Beck, C.R. et al. (2010) LINE-1 retrotransposition activity in human genomes. *Cell*, **141**, 1159–1170.
- Bennett, E.A. et al. (2008) Active alu retrotransposons in the human genome. *Genome Res.*, **18**, 1875–1883.
- Brawand, D. et al. (2011) The evolution of gene expression levels in mammalian organs. *Nature*, **478**, 343–348.
- Bundo, M. et al. (2014) Increased L1 retrotransposition in the neuronal genome in schizophrenia. *Neuron*, **81**, 306–313.
- Chung, D. et al. (2011) Discovering transcription factor binding sites in highly repetitive regions of genomes with multi-read analysis of ChIP-Seq data. *PLoS Comput. Biol.*, **7**, e1002111.
- Coufal, N.G. et al. (2009) L1 retrotransposition in human neural progenitor cells. *Nature*, **460**, 1127–1131.
- Coufal, N.G. et al. (2011) Ataxia telangiectasia mutated (ATM) modulates long interspersed element-1 (L1) retrotransposition in human neural stem cells. *Proc. Natl. Acad. Sci.*, **108**, 20382–20387.
- Criscione, S. et al. (2014) Transcriptional landscape of repetitive elements in normal and cancer human cells. *BMC Genomics*, **15**, 583.
- Day, D.S. et al. (2010) Estimating enrichment of repetitive elements from high-throughput sequence data. *Genome Biol.*, **11**, R69.
- De Cecco, M. et al. (2013) Transposable elements become active and mobile in the genomes of aging mammalian somatic tissues. *Aging*, **5**, 867–883.
- Dobin, A. et al. (2012) STAR: ultrafast universal RNA-seq aligner. *Bioinformatics*, **29**, 15–21.
- Fadloun, A. et al. (2013) Chromatin signatures and retrotransposon profiling in mouse embryos reveal regulation of LINE-1 by RNA. *Nat. Struct. Mol. Biol.*, **20**, 332–338.

- Faulkner, G.J. *et al.* (2009) The regulated retrotransposon transcriptome of mammalian cells. *Nat. Genet.*, **41**, 563–571.
- Gnanakkan, V.P. *et al.* (2013) TE-array—a high throughput tool to study transposon transcription. *BMC Genomics*, **14**, 869.
- Griebel, T. *et al.* (2012) Modelling and simulating generic RNA-seq experiments with the flux simulator. *Nucleic Acids Res.*, **40**, 10073–10083.
- Han, B.W. *et al.* (2015) piPipes: a set of pipelines for piRNA and transposon analysis via small RNA-seq, RNA-seq, degradome- and CAGE-seq, ChIP-seq and genomic DNA sequencing. *Bioinformatics*, **31**, 593–595.
- Hancks, D.C. and Kazazian, H.H., Jr. (2012) Active human retrotransposons: variation and disease. *Curr. Opin. Genet. Dev.*, **22**, 191–203.
- Honma, M.A. *et al.* (1993) High-frequency germinal transposition of DsALS in Arabidopsis. *Proc. Natl. Acad. Sci.*, **90**, 6242–6246.
- Huang, C.R. *et al.* (2012) Active transposition in genomes. *Annu. Rev. Genet.*, **46**, 651–675.
- Jurka, J. *et al.* (2005) Repbase update, a database of eukaryotic repetitive elements. *Cytogenet. Genome Res.*, **110**, 462–467.
- Kano, H. *et al.* (2009) L1 retrotransposition occurs mainly in embryogenesis and creates somatic mosaicism. *Genes Dev.*, **23**, 1303–1312.
- Karolchik, D. *et al.* (2003) The UCSC genome browser database. *Nucleic Acids Res.*, **31**, 51–54.
- Kelley, D. and Rinn, J. (2012) Transposable elements reveal a stem cell-specific class of long noncoding RNAs. *Genome Biol.*, **13**, R107.
- Lamprecht, B. *et al.* (2012) Derepression of an endogenous long terminal repeat activates the CSF1R proto-oncogene in human lymphoma. *Nat. Med.*, **16**, 571–579.
- Langmead, B. *et al.* (2009) Ultrafast and memory-efficient alignment of short DNA sequences to the human genome. *Genome Biol.*, **10**, R25.
- Lee, E. *et al.* (2012) Landscape of somatic retrotransposition in human cancers. *Science*, **337**, 967–971.
- Li, H. *et al.* (2009) The sequence alignment/map format and SAMtools. *Bioinformatics*, **25**, 2078–2079.
- Li, W. *et al.* (2012) Transposable elements in TDP-43-mediated neurodegenerative disorders. *PLoS One*, **7**, e44099.
- Li, W. *et al.* (2013) Activation of transposable elements during aging and neuronal decline in drosophila. *Nat. Neurosci.*, **16**, 529–531.
- Lu, X. *et al.* (2014) The retrovirus HERVH is a long noncoding RNA required for human embryonic stem cell identity. *Nat. Struct. Mol. Biol.*, **21**, 423–425.
- Macia, A. *et al.* (2011) Epigenetic control of retrotransposon expression in human embryonic stem cells. *Mol. Cell Biol.*, **31**, 300–316.
- Mills, R.E. *et al.* (2007) Which transposable elements are active in the human genome? *Trends Genet.*, **23**, 183–191.
- Molaro, A. *et al.* (2014) Two waves of de novo methylation during mouse germ cell development. *Genes Dev.*, **28**, 1544–1549.
- Muotri, A.R. *et al.* (2005) Somatic mosaicism in neuronal precursor cells mediated by L1 retrotransposition. *Nature*, **35**, 903–910.
- Nussbaumer, T. *et al.* (2013) MIPS PlantsDB: a database framework for comparative plant genome research. *Nucleic Acids Res.*, **41**, 1144–1151.
- Ohnuki, M. *et al.* (2014) Dynamic regulation of human endogenous retroviruses mediates factor-induced reprogramming and differentiation potential. *Proc. Natl. Acad. Sci.*, **111**, 12426–12431.
- Ohtani, H. *et al.* (2013) DmGTSF1 is necessary for Piwi-piRISC-mediated transcriptional transposon silencing in the drosophila ovary. *Genes Dev.*, **27**, 1656–1661.
- Peaston, A.E. *et al.* (2004) Retrotransposons regulate host genes in mouse oocytes and preimplantation embryos. *Dev. Cell*, **7**, 597–606.
- Perrat, P.N. *et al.* (2013) Transposition-driven genomic heterogeneity in the drosophila brain. *Science*, **340**, 91–95.
- Reilly, M.T. *et al.* (2013) The role of transposable elements in health and diseases of the central nervous system. *J. Neurosci.*, **33**, 17577–17586.
- Rosenfeld, J.A. *et al.* (2009) Investigating repetitively matching short sequencing reads: the enigmatic nature of H3K9me3. *Epigenetics*, **4**, 476–486.
- Rozhkov, N. *et al.* (2013) Multiple roles for Piwi in silencing drosophila transposons. *Genes Dev.*, **27**, 400–412.
- Sciamanna, I. *et al.* (2013) A tumor-promoting mechanism mediated by retrotransposon-encoded reverse transcriptase is active in human transformed cell lines. *Oncotarget*, **4**, 2271–2287.
- Sciamanna, I. *et al.* (2014) Regulatory roles of LINE-1-encoded reverse transcriptase in cancer onset and progression. *Oncotarget*, **5**, 8039–8051.
- Sedivy, J.M. *et al.* (2013) Death by transposition—the enemy within? *Bioessays*, **35**, 1035–1043.
- Shukla, R. *et al.* (2013) Endogenous retrotransposition activates oncogenic pathways in hepatocellular carcinoma. *Cell*, **153**, 101–111.
- Smit, A. *et al.* (1996–2010) Repeatmasker Open-3.0, <<http://www.repeatmasker.org>>.
- Thomas, C.A. *et al.* (2012) LINE-1 retotransposition in the nervous system. *Annu. Rev. Cell Dev. Biol.*, **28**, 555–573.
- Trapnell, C. *et al.* (2010) Transcript assembly and quantification by RNASeq reveals unannotated transcripts and isoform switching during cell differentiation. *Nat. Biotech.*, **28**, 511–515.
- Trapnell, C. *et al.* (2012) Differential gene and transcript expression analysis of RNA-seq experiments with TopHat and cufflinks. *Nat. Protocols*, **7**, 562–578.
- Treangen, T.J. and Salzberg, S.L. (2011) Repetitive DNA and next-generation sequencing: computational challenges and solutions. *Nat. Rev. Genet.*, **13**, 36–46.
- Tubio, J.M. *et al.* (2014) Extensive transduction of nonrepetitive DNA mediated by L1 retrotransposition in cancer genomes. *Science*, **345**, 1251343.
- Tucker, B.A. *et al.* (2011) Exome sequencing and analysis of induced pluripotent stem cells identify the cilia-related gene male germ cell-associated kinase (MAK) as a cause of retinitis pigmentosa. *Proc. Natl. Acad. Sci.*, **108**, E569–E576.
- Varadhan, R. and Roland, C. (2008) Simple and globally convergent methods for accelerating the convergence of any EM algorithm. *Scand. J. Stat.*, **35**, 335–353.
- Wang, J. *et al.* (2010) A Gibbs sampling strategy applied to the mapping of ambiguous short-sequence tags. *Bioinformatics*, **26**, 2501–2508.
- Wang, J. *et al.* (2014) Primate-specific endogenous retrovirus-driven transcription defines naive-like stem cells. *Nature*, **516**, 405–409.